On the Stability of the Near-Earth Magnetotail at Growth Phase

P. Dobias[1], J. A. Wanliss[2], I. O. Voronkov[1], and J. C. Samson[1]

[1]Department of Physics, University of Alberta, Edmonton, Alberta, T6G 2J1, Canada

[2]Embry-Riddle Aeronautical University 600 S. Clyde Morris Blvd, Daytona Beach 32114, USA

Keywords: nonlinear plasma instabilities, substorms, energy principles

ABSTRACT

During a growth phase of a magnetospheric substorm the near-Earth magnetotail stretches and thins, remaining in the near-equilibrium state. We use a stability analysis, based on the comparison of energy density terms, to test stability of observation-constrained equilibrium configurations corresponding to the Earth's magnetic field at various stages of the substorm growth phase prior to onset. We demonstrate that during the growth phase of a substorm the near-Earth plasma sheet is nonlinearly stable, preventing any large-scale instabilities. However, at the time just prior to onset, the system becomes unstable to a large scale, nonlocal, explosive (with growth rate increasing with time) instability. Possible triggering mechanisms could include field line resonances (FLRs), localized linear instabilities (linear ballooning, KH-modes, etc.), or strong convection pulses. Our results suggest that the substorm onset starts close to the Earth (around 10 R_E) as a large-scale explosive instability that brings about reconfiguration of the entire system.

1 INTRODUCTION

Dobias et al. [2004] developed a method of stability analysis for magnetized plasmas based on the behavior of potential energy density [Pfirsch and Sudan, 1993; Dobias and Samson, 2004]. These methods have a long tradition in various areas of fluid dynamics and plasma physics [Bernstein et al, 1958; Low, 1958; Arnold, 1969]. Dobias et al. presented an example of the stability analysis in the case of artificial equilibrium configurations resembling the magnetospheric configuration at late substorm growth phase. Their analysis suggested a possible explanation of some substorm features such as an occurrence of one or more pseudobreakups, formed from preexisting auroral arcs near the equatorward edge of the auroral region.

In the present work we have developed the analysis of Dobias et al. further. We use a 3-dimensional equilibrium based on the Grad-Shafranov equation and constrain the equilibrium by CANOPUS observations to obtain a profile of the plasma pressure and magnetic field during the later stages of the substorm growth phase, just prior to onset. We use a field line resonance (FLR) type of plasma perturbation to test the stability of the magnetospheric configurations, because they can be easily generated in the near-Earth plasma sheet by a variety of different mechanisms [Samson et al., 1996; Samson et al., 2003, Voronkov et al., 2004]. The fast 180º-phase shift in the azimuthal component of the plasma displacement associated with a resonance seems to be an important factor contributing to the destabilizing of the plasma system. It is consistent with the fact that an occurrence of a resonant coupling in dynamical systems [Marsden and Ratiu, 1999; Cherry, 1959; Cherry, 1968] can cause a destabilization of dynamical systems. Thus we provide a connection between ground-based observations of the substorms and the nonlinear stability analysis of the earthward edge of the plasma sheet at about 10-12 R_E.

2 EQUILIBRIUM CONSTRAINED BY OBSERVATIONS

The plasma equilibrium is described by the Grad-Shafranov equation

$$\frac{{}^{2}}{r^{2}} + \frac{\sin}{r^{2}} \frac{}{} \frac{1}{\sin} \frac{}{} = 4\ {}^{2}\ {}_{0}\sin^{2} \frac{P}{}, \qquad (1)$$

with magnetic field defined as

$$\boldsymbol{B} = \frac{1}{2} \quad . \qquad (2)$$

The radius r, polar angle , and azimuthal angle are spherical coordinates; and the plasma pressure $P(\ )$ is a function of the flux .

To construct a 3-dimensional equilibrium we sum the dipole field solution, valid for the constant pressure gradient, and a second solution, valid when the plasma pressure is a linear function of the magnetic flux. Then the flux function can be expressed as

$$(r,\ ) = 2\ \frac{M\sin^2}{r}\ \ 1+\frac{1}{2}\ \ \frac{r}{R_X}^{3}+\ +\frac{}{4}\ \ \frac{r}{R_X}^{5}+\ +\ + , \qquad (3)$$

where M is the magnetic moment for the Earth's dipole field,   accounts for the pressure gradient, and R_X is the radial position of the equatorial x-line in the magnetic field.

We use expression (3) combined with CANOPUS observations to obtain equilibrium magnetospheric configurations at various stages of the growth phase. For our analysis we have chosen the February 9, 1995 substorm with onset around 04:35 UT (Fig1). For more details on this event see [Friedrich et al., 2001].

The modeling approaches followed by Wanliss et al. [2000, 2002] have successfully reproduced reasonable current sheet thicknesses during substorms. Our method of evaluating the magnetic field topology stems from the observations of low-altitude isotropy boundaries of precipitating particles. The concept of using the isotropy boundaries for remote sensing of the magnetotail topology was first introduced by Sergeev and Malkov [1988] and further developed by others [Sergeev et al., 1993; Pulkkinen et al., 1991, 1992, 1998; Kubyshkina et al., 1999; Donovan et al., 2003]. The technique relies on the inference that the isotropy boundaries of precipitating particles observed at low altitudes correspond to the boundaries between adiabatic and nonadiabatic regimes of particle motion in the equatorial current sheet region. Scattering out of the current sheet depends on the equatorial magnetic field topology and is also sensitively dependent on the gyroradius of the particle. The theory of scattering out of the plasma sheet and subsequent precipitation has been described in numerous other papers [Buchner and Zelenyi, 1987; Zelenyi et al., 1990; Liu et al., 1998]. Basically, when there exists significant spatial magnetic field variations on the scale of the particle gyroradius, nonadiabatic behavior occurs with the result of scattering out of the plasma sheet. Knowledge of the particular magnetic topology and particle energy profile allows one to calculate the isotropy boundary in the magnetotail.

The original aspect of the work by Wanliss et al. extends the isotropy boundary idea to include the ground observations of the meridian scanning photometers. The equatorward boundary of diffuse H- emissions form a sharp boundary delineating the ionospheric regions between isotropic precipitating particle and trapped particle distributions [Samson, 1994; Donovan et al., 2003]. Thus they were able to make a direct connection between the remote magnetic topology and the ground-based data. Although successful, and designed by careful comparison of averaged magnetic fields in the lobe and plasma sheet regions during different stages of magnetospheric activity, the models introduced by Wanliss et al. [2000, 2002] were essentially ad hoc. In the present work we follow these models combined with a different approach that utilizes the more physically appropriate equilibrium magnetotail model. We iterate the equilibrium model and varying the two free parameters (pressure and a position of the magnetic X-line) to minimize, in a least squares sense, the latitudinal difference between the ground-based photometer isotropy boundary and the model prediction. We also assume that the energy of precipitating protons at the isotropy boundary is 20 keV.

3 NONLINEAR STABILITY ANALYSIS OF THE NEAR-EARTH PLASMA SHEET

Our stability analysis method was suggested by Pfirsh and Sudan [1993] and further developed by Dobias and Samson [2004]. It is based on comparison of the higher order terms in the expansion of potential energy density in terms of plasma displacement. Energy density can be expanded in powers of plasma displacement [Dobias et al., 2004]. A dominant second order term in potential energy means that the system can be described within a linear approximation. The third and the fourth order terms can be used to determine possible nonlinear stability properties of the system. If the third order term is dominant, then the system is explosively (with the growth-rate increasing with time) unstable. If the fourth order term dominates, nonlinear saturation occurs, and the system evolves to a non-linearly stable state [Pfirsch and Sudan, 1993; Fong et al., 1999; Dobias et al., 2004].

For the analysis we use a plasma displacement functions

$$_r = {}_{r0} \ln\left(x \quad x_r + i \quad\right) \qquad (4)$$

for the radial, and

$$= \frac{_0}{x \quad x_r \quad i} \qquad (5)$$

for the azimuthal component of the plasma displacement (Fig. 2) in the equatorial plane. x_r is the position of the resonance, is a small parameter that prevents singularity.

The analysis goes as follows. For selected magnetospheric configurations we calculate energy density expansion terms using plasma displacement (4) and (5). Then we compare relative values of the magnitude of the energy density to find out if the system is stable or unstable. We start with a small value of the plasma displacement magnitude to keep the ordering $^{(2)} >> {}^{(3)} >> {}^{(4)}$ ($^{(a)}$ denotes the a-th order in the potential energy density). Then we slowly increase magnitude of the plasma displacement until the plasma displacement triples. This way we are able to analyze a transition from linear to nonlinear behavior. If the fourth order term becomes dominant before the third order term reaches its dominance, such a system is nonlinearly stable. However, if the increase in the magnitude of the displacement preserves dominance of the third order term the system is explosively unstable and a large-scale reconfiguration of the system (dipolarization) is possible. Generally speaking, the scale at which we can increase the magnitude of the plasma displacement yields a possible room for the growth of instability before it is saturated.

We tested nonlinear stability of magnetosphere at various stages of the February 9, 1995 substorm. The substorm expansion started around 4:35UT (Fig. 1). We have performed our tests at 4:20, 4:30, and 4:35 UT. We started each of the tests with the magnitude of the azimuthal displacement of 0.5 R_E and increased it all the way to 2 R_E to analyze a possible room for the growth of the instability before it saturated due to nonlinear effects. Figures 3 and 4 show the energy densities in the equatorial plane at 4:20 UT and 4:30 UT for the displacements 0.5, 0.6, and 1 R_E. In both situations the fourth order term becomes dominant (nonlinear saturation) after a small increase in the magnitude of the plasma displacement. It means that both these configurations are stable. However, in the case of the 4:30 UT configuration we can see that the third order term gains importance, and the system is quickly approaching a threshold of instability.

Figure 5 shows energy densities for the 4:35 UT configuration. The magnitudes of the plasma displacement were in this case 0.5, 1, and 2 R_E. Note that despite an increase in the plasma displacement from 1 to 2 R_E the system is still explosively unstable. It means that for this configuration a large-scale explosive instability causing reconfiguration of the whole system is possible.

5 CONCLUSION

Using an energy-based stability analysis outlined in [Dobias et al., 2004] we have tested the nonlinear stability of the near-Earth edge of the plasma sheet during the late growth phase of the February 9, 1995 substorm. We used the Grad-Shafranov equation to calculate equilibrium configurations of the magnetosphere. This equilibrium was constrained by the CANOPUS data to match the theoretical equilibrium to the real magnetosphere as closely as possible. Assuming a presence of a resonant type of perturbation in the auroral region [Samson et al., 2003; Voronkov et al., 2004] we calculated perturbation energy densities up to the fourth order in the plasma displacement in the magnetosphere at 4:20, 4:30, and 4:35UT. The first two configurations, corresponding to the late growth phase were nonlinearly stable. However, the last configuration corresponding approximately to the time of onset as seen in the CANOPUS data, was unstable, allowing for significant growth of the nonlinear instability.

To summarize our results, we showed that during the February 9, 1995 substorm the near-Earth edge of the plasma sheet was stable during the growth phase. Only at the time corresponding approximately to the onset did it become nonlinearly unstable. Thus we can speculate that this onset was caused by a large-scale explosive instability in the near-Earth plasma sheet. Further analysis needs to include a possibility of the occurrence of the shear-flow instability in the resonant region. The strong shear caused by the resonant type profiles is very likely to generate shear-flow instability [Voronkov et al., 1997] and thus this possibility needs to be incorporated into further stability analysis. Also, at this stage additional effects such as Hall and kinetic, and a possible influence of the external parameters may be of an interest to be considered.

ACKNOWLEDGMENTS

This research was funded by the Natural Sciences and Engineering Research Council (NSERC) of Canada and by the Canadian Space Agency (CSA). CANOPUS is an array funded by the CSA.

REFERENCES

[1] Arnold, V. I., On an a priori estimates in the theory of hydrodynamical stability, *Amer. Math. Soc. Transl.*, **79**, 267, 1969.

[2] Bernstein, I. B., E. A. Frieman, M. D. Kruskal, R. M. Kulsrud, An energy principle for hydromagnetic stability problems, *Proc. R. Soc. London*, **A17**, 244, 1958.

[3] Büchner, J., and L. M. Zelenyi, Chaotization of the electron motion as the cause of an internal magnetotail instability and the substorm onset, *J. Geophys. Res.*, **92**, 13,456, 1987.

[4] Cherry, T. M., The pathology of differential equations, *J. Austral. Math. Soc.*, **1**, 1, 1959.

[5] Cherry, T. M., Asymptotic solution of analytic Hamiltonian systems, *J. Differential Equations*, **4**, 142, 1968.

[6] Dobias P. and J. C. Samson, Nonlinear instabilities in magnetized plasmas: A geometrical treatment, *Can. J. Phys.*, accepted, 2004.

[7] Dobias, P., I. O. Voronkov, J. C. Samson, On nonlinear plasma instabilities during the substorm expansive phase onset, *Phys. Plasmas*, **11**, 2046, 2004.

[8] Donovan, E. F., B. J. Jackel, I. Voronkov, T. Sotirelis, F. Creutzberg, and N. A. Nicholson, Ground-based optical determination of the b2i boundary: A basis for an optical MT-index, *J. Geophys. Res.*, **108**, 1115, 2003.

[9] Fong, B. H., S. C. Cowley, O. A. Hurricane, Metastability of magnetically confined plasmas, *Phys. Rev. Lett.*, **82**, 4651, 1999.

[10] Friedrich, E., J. C. Samson, I. Voronkov, G. Rostoker, Dynamics of the substorm expansive phase, *J. Geophys. Res.*, **106**, 13145, 2001.

[11] Kubyshkina, M. V., V. A. Sergeev, and T. I. Pulkkinen, Hybrid input algorithm: An even-oriented magnetospheric model, *J. Geophys. Res.*, **104**, 24,977, 1999.

[12] Low, F. E., A Lagrangian formulation of the Boltzman-Vlasov equation for plasmas, *Proc. Roy. Soc. London*, **A248**, 282, 1958.

[13] Liu, W. W., G. Rostoker, and J. C. Samson, Precipitation of hot protons from a stretched near-Earth current sheet, *COSPAR Colloq. Ser.*, **9**, 165, 1998.

[14] Marsden, J. E., T. S. Ratiu, *Introduction to mechanics and symmetry*, Springer-Verlag, 1999.

[15] Pfirsch, D., and R. N. Sudan, Nonlinear ideal magnetohydrodynamic instabilities, *Phys. Fluids*, **7**, 2052, 1993.

[16] Pulkkinen, T. I., et al., Modeling the growth phase of a substorm using the Tsyganenko model and multi-spacecraft observations: CDAW-9, *Geophys. Res. Lett.*, **18**, 1963, 1991.

[17] Pulkkinen, T. I., D. N. Baker, R. J. Pellinen, J. Büchner, H. E. J. Koskinen, R. E. Lopez, R. L. Dyson, and L. A. Frank, Particle scattering and current sheet stability in the geomagnetic tail during the substorm growth phase, *J. Geophys. Res*., **97**, 19,283, 1992.

[18] Pulkkinen, T. I., D. N. Baker, L. L. Cogger, T. Mukai, and H. J. Singer, Coupling of inner tail and midtail processes, in: *Substorms-4*, edited by S. Kokubun and Y. Kamide, p. 749, Terra Sci., Tokyo, 1998.

[19] Samson, J. C., Mapping substorm intensifications from the ionosphere to the magnetosphere, in: *Proceedings of the International Conference on Substorms 2*, edited by J. R. Kan, J. D. Craven, and S. I. Akasofu, p. 189, Univ. of Alaska, Fairbanks, 1994.

[20] Samson, J. C., L. L. Cogger, Q. Pao, Observations of field line resonances, auroral arcs, and auroral vortex structures, *J. Geophys. Res*., **101**, 17373, 1996.

[21] Samson, J. C., R. Rankin, V. T. Tikhonchuk, Optical signatures of auroral arcs produced by field line resonances; comparison with satellite observations and modeling, *Annales Geophysicae*, **21**, 933, 2003.

[22] Sergeev, V. A., and M. V. Malkov, Diagnostics of the magnetic configuration of the plasma layer from measurements of energetic electrons above the ionosphere, *Geomagn. Aeron*., **28**, 549, 1988.

[23] Sergeev, V. A., D. G. Mitchell, C. T. Russell, and D. J. Williams, Structure of the tail plasma/current sheet at 11 RE and its changes in the course of a substorm, *J. Geophys. Res*., **98**, 17,345, 1993.

[24] Voronkov, I., R. Rankin, P. Frytz, V. T. Tikhonchuk, J.C. Samson, Coupling of shear flow and pressure gradient instabilities, *J. Geoph. Res*., **102**, 9639, 1997.

[25] Voronkov, I. O., et al., Late growth phase and breakup in the near-Earth plasma sheet, in: *Proceedings of the 7th International Conference on Substorms*, 2004.

[26] Wanliss, J. A., J. C. Samson, E. Friedrich, On the use of photometer data to map dynamics of the magnetotail current sheet during substorm growth phase, *J. Geophys. Res*., **105**, 27673, 2000.

[27] Wanliss, J. A., R. Rankin, J. C. Samson, V. T. Tikhonchuk, Field line resonances in a stretched magnetotail: CANOPUS optical and magnetometer observations, *J. Geophys. Res*., **107**, 10.1029, 2002.

[28] Zelenyi, L., A. Galeev, and C. F. Kennel, Ion precipitation from the inner plasma sheet due to stochastic diffusion, *J. Geophys. Res*., **95**, 3871, 1990.

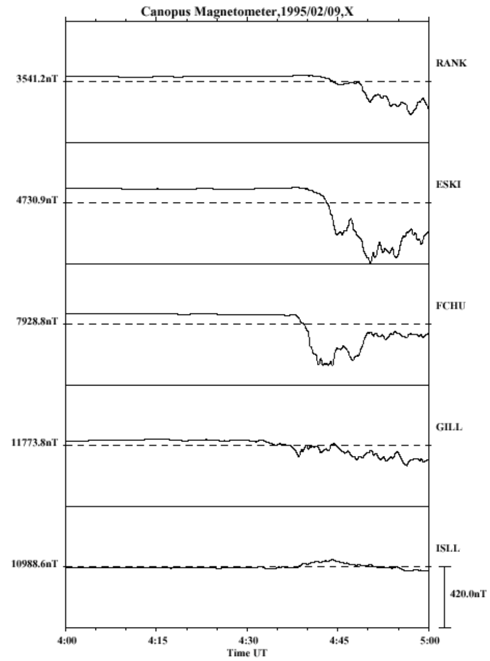

Figure 1 CANOPUS magnetometer data for Feb 9, 1995. The substorm starts around 4:35 UT.

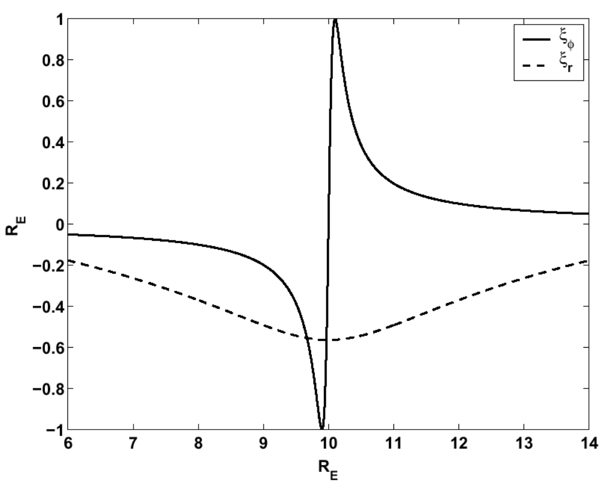

Figure 2 Radial and azimuthal component of plasma displacement

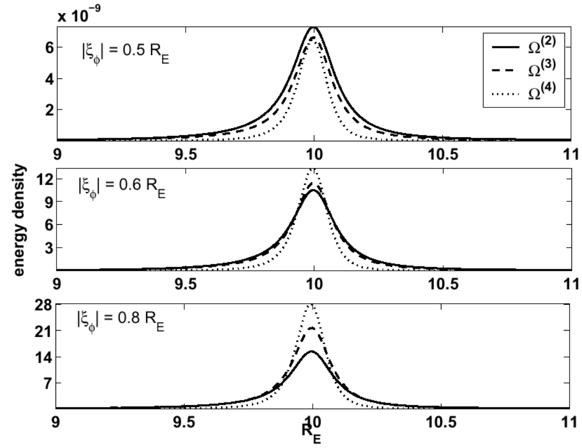

Figure 3 Normalized energy densities (( )) in the equatorial plane for various magnitudes of the plasma displacement at 4:20 UT. Superscript denotes order in the expansion.

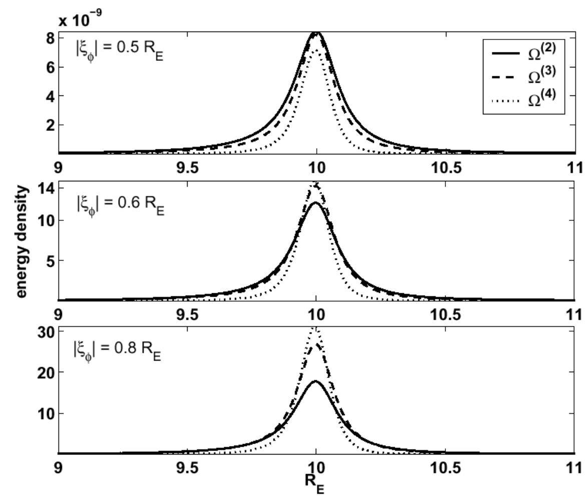

Figure 4 Normalized energy densities (( )) in the equatorial plane for various magnitudes of the plasma displacement at 4:30 UT. Superscript denotes order in the expansion.

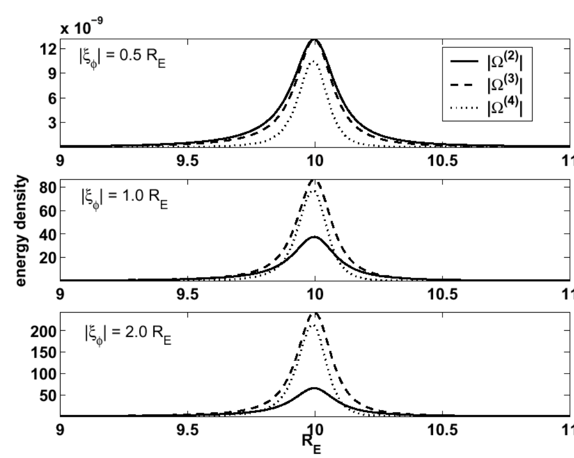

Figure 5 Normalized energy densities (( )) in the equatorial plane for various magnitudes of the plasma displacement at 4:35 UT. Superscript denotes order in the expansion.